International Journal of Scientific Research and Engineering Development-– Volume 4 Issue 4, July- Aug 2021

Available ***www.ijsred.com***

OPEN ACCESS RESEARCH ARTICLE

OPTIMUM DESIGN OF VERTICAL RECTANGULAR FIN ARRAY

Hamza Mohamed[*], J.El-shiba, and Emad Omar Elwahab[**]

*(Mechanical Power Engineering Department, University of Gharian,Faculty of Engineering, Libya. Email: hmzamohamed71@gmail.com)

*(Mechanical and Industry Engineering Department, Elmergib University, Faculty of Engineering, Libya. Email: eoelwahab@elmergib.edu.ly)

ABSTRACT

Experimental and numerical investigations have been performed to study the natural convection heat transfer from a vertical rectangular fin arrays at different orientation angles.An experimental set-up was constructed and calibrated to test different fin configurations. It basically consists of base plate, an array of parallel longitudinal fins, heating unit and layers of thermal insulation. Fin length (L) and fin thickness (t) were kept fixed at 187 and 6.5 mm respectively, while fin spacing (S) was varied from 3 to 16 mm and fin height (H) was varied from 15 to 45 mm. The orientation angle (β) was changed from 0° to 60°, and temperature difference between fin and surrounding (ΔT) from 30 to 95°C.Base-to-ambient temperature difference was also varied through a calibrated wattmeter ranging from 10 to 180W. To understand the general flow patterns dominating flows from the heat sink, the three-dimensionless elliptic governing equations were solved using finite volume computational fluid dynamics (CFD) code. A comparative study between the experimental and numerical results was performed to verify the numerical code. It was found for the configuration tested that the heat transfer rate per unit base area increases with the increase in the fin spacing and reaches a maximum value then decreases with farther increase in the fin spacing. The maximum heat dissipation occurs at optimal spacing S_{opt}=7 mm. Empirical correlations between Nussult number, Rayleigh number, fin spacing, fin height, orientation angle, temperature difference between the fin and surroundings were derived. Finally the present work general empirical formula is given in the form

$$Nu_L = 50.08 \left[Ra_L \frac{(S)}{H}\right]^{-6.8229E-05} \left(\frac{L}{H}\right)^{1.04E-07} \left(\frac{L}{S}\right)^{5.12E-10} Cos\beta^{1.1E-06}$$

Where , 15 mm ≤ H ≤ 45 mm, 3mm ≤ S ≤ 16 mm, °0 ≤ β ≤°60, t = 6.5 mm, L = 187 mm.

Keywords: Hat transfer; Laminar flow; Numerical simulation; Free convection.

الملخص العربي

في هذا البحث أجريت مجموعة من التجارب المعملية والدراسات النظرية على أداء انتقال الحرارة بالحمل من مصفوفة من الزعانف العمودية المستطيلة عند زوايا ميل مختلفة. لهذا الغرض تم تصنيع جهاز لإجراء التجارب المعملية ومعايرته لاختبار تكوينات الزعانف المختلفة. والذي يتكون من قاعدة مستوية ومجموعة من الزعانف الطولية ووحدة تسخين وطبقات من العزل الحراري. لقد تم تثبيت كل من طول الزعانف و كذلك سمكها عند 187 مم و 6.5 مم , وإثناء التجارب كانت المسافة بين الزعانف تتراوح بين 3 إلى 16 ممبينما كان ارتفاع الزعانف يتراوح بين 15 إلى 45 ممكانت زاوية ميل الزعانف تتغير من 0 إلى 60 درجة. وكان الفرق في درجات الحرارة بين الزعانف والهواء المحيط بها تتراوح بين 30 إلى 95 درجة مئوية. كذلك تباينت فروق درجات الحرارة و دلك من خلال الوات متر الذي تم معايرته لتتراوح من 10 إلى 180 وات. ولفهم طبيعة انتقال الحرارة والسريان من الزعانف عند زوايا الميل المختلفة تم حل المعادلات الحاكمة في ثلاث اتجاهات باستخدام طريقة الحجم المحدود. ووجد من التجارب أن معدل انتقال الحرارة لكل وحدة مساحة من القاعدة يزداد مع زيادة المسافة بين الزعانف إلى أن يصل إلى أقصى قيمة له ثم ينقص مع أي زيادة أخرى في المسافة بين

الزعانف. وكان أقصى فقد حراريى يمكن ازالته من الزعانف عند مسافة مثالية قدرها 7مم. أيضا تم استنتاج معادلات تجريبية تربط بين عدد نسلت وعدد رايلى والمسافة بين الزعانف وطول الزعانف وزاوية الميل والفرق في درجات الحرارة بين الزعانف و الهواء المحيط بها.وأخيرا ونظرا للعمل العام الحالي تم وضع الصيغة في الشكل

$$Nu_L = 50.08\left[Ra_L\frac{(S)}{H}\right]^{-6.8229E-05}\left(\frac{L}{H}\right)^{1.04E-07}\left(\frac{L}{S}\right)^{5.12E-10}Cos\beta^{1.1E-06}$$

حيث أن 15 mm ≤ H ≤ 45 mm, 3mm ≤ S ≤ 16 mm, °0 ≤ β ≤°60, t = 6.5 mm, L = 187 mm.

NOMENCLATURE			
A	Total heat transfer area (m^2)	t	fin thickness, m
CFD	Computational fluid dynamics	T	Temperature, k
g	gravitational acceleration, m/s^2	T_s	Temperature of the surface, k
h	convection heat transfer coefficient, $w/m^2.k$	x,y,z	rectangular coordinates, m
H	fin height, m	**Greek Letters**	
k	thermal conductivity, w/m.k ; Boltzmann's constant	α	thermal diffusivity, m^2/s
L	based on characteristic length ; fin length, m	ε	Emissivity
N	Number of temperature increments in a flux plot	ε_f	fin effectiveness
Nu	Nusselt Number	η_f	fin efficiency
L_c	characteristic length, m	η_o	fin temperature effectiveness
q	Heat transfer rate, w	θ	Temperature deference, k
$\dot{q}$	power input to the heater, w	μ	viscosity, kg/m.s
q"	Heat flux, w/m^2	ν	Kinematic viscosity, m^2/s
Ra	Rayleigh Number	ρ	mass density, kg/m^3
R_t	thermal resistance, k/w	σ	Stefan-Boltzmann constant, $w/m^2.k^4$
$R_{t,f}$	fin thermal resistance	Φ	Orientation angel
$R_{t,o}$	Thermal resistance of fin array, k/w	Δ	Difference
S	shape factor of two-dimensional conduction, m ; fin spacing, m	β	volumetric thermal expansion coefficient, k^{-1} ; orientation angel, degree

1. INTRODUCTION

Heat removal in an efficient way is necessary in order to maintain reliable operation of electronic devices and solar energy applications to cooling of nuclear reactor fuel elements. For an efficient application of natural convection to cooling processes it is necessary to fully understand the mechanisms involved in the free-convection cooling of electronic and thermoelectric devices.

The use of natural convection air-cooling extended surfaces provides a reliable, cheap and widely used method of cooling for dissipating unwanted heat. Besides, their design is simple, economic and without any acoustic noise, the convective heat transfer from an extended surface can be increased either by increasing heat transfer coefficient or the surface area or both of these quantities. Increasing the heat transfer area is preferred as the simplest method to

enhance heat dissipation rate, because the use of better fluid to increase the heat transfer coefficient is not an economical and practical solution. The only the controllable variable to enhance the convective heat transfer rate from an extended surface is the geometry of the fins.

Burak, et al.[3], investigated the optimal fin spacing for vertical rectangular fins protruding from a vertical rectangular base. ***V. Dharma Rao et al***.[4], went on to study the problem of laminar natural convection heat transfer from a fin array containing a vertical base and horizontal fins is theoretically formulated by treating the adjacent internal fins as two fin enclosures. ***R.L. Edlabadkaret al.***[5], reported an experimental work on enhancement of natural convection heat transfer from vertical plate with a horizontal partition plate and V-plates in water as ambience.***Arularasan R et al***.[7].

Although many previous researches were made towards the understanding of natural convection from fin arrays, nearly no experimental and numerical data are available for the longitudinal fins which are also a very popular fin configuration used for electronic cooling and others applications. In particular, few researches have explicitly demonstrated the subtle difference of orientation effect on the fin performance, which is of practical importance for relevant applications. For this reason, the first object of this study is to provide experimental and numerical data for longitudinal fin heat sink under natural convection. Secondly, the dependence of longitudinal fin performance on the orientation effect is presented in a more detailed manner.

2. EXPERIMENTAL SET UP

The set-up primarily consists of a base plate with a supporting frame on which the fin-arrays are mounted, and various instruments for measuring the ambient temperature, base-plate temperature and the input power forthe heater. A schematic view of the experimental set-up is presented in *Figure 1.*

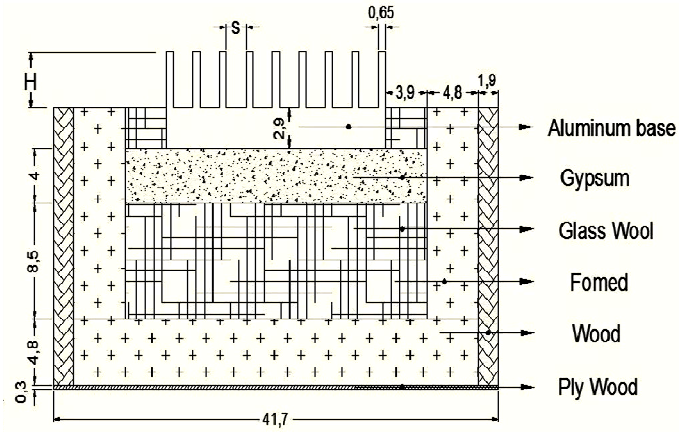

Figure 1. Schematic diagram of the Testing device.

The tested model (*heat sink*) consists of square base plate, tested fins, and heating unit, they of assembled together by wooden container with dimensions were 417 *mm* wide, 390 *mm* long and 205 *mm* height as shown in *Figure 1.* The base plate is made from pure aluminum metal, with 187 *mm* long using the durmetal adhesive with K (0.758 w/m.k). During the experiments, the fin height (H), the fin thickness (t), the inter-fin space (S) and the fins number (N) were varied as shows in *Table 1*, and the rotating angle β is (0°,30° and 60°), 205 *mm* wide and 29 *mm* high. The tested fins are made from the same metal of the base plate. The fins are of rectangular type with (t) wide, (H) high and (L) long rectangular fins of 6.5 *mm* wide, 187 *mm* length and with different highs. Eight copper-constantan type (T) and two nickel chrome type (k) thermocouples were distributed uniformly along each side to measure the temperature

distribution through the fins. The fins are mounted on the base plate, with inter-fin spacing (S) (the distance between of two adjacent fins) by

Table 1 Geometrical parameters used in the experiment

Fin thickness t (*mm*)	Fin height H (*mm*)	Fin spacing S (*mm*)
6.5	15	3
6.5	35	6.5
6.5	45	16

The heating unit mainly consists of the main electric heater and the thermal insulation. The heater output power of is 1210 W at 220 V. The electrical power input to the heater was controlled by a variac transformer to obtain constant heat flux along the base plate and measured by an in-line digital wattmetershown in*Figure (2)*, eight thermocouples were distributed in the center points of the inner and the outer surfaces of the insulation boards to measure the temperatures and calculate the heat losses through the insulation layers. The readings of thermocouples were taken out by two digital thermometers shown in the*Figure (3).*Voltage inputs and supplies current to the heater are also measured as well, and calculated energy inputs can be verified by the digital multi-meter readings,shown in the *Figure. (4)*.

Figure 2. Digital thermometer.

Figure 3. Digital Watt Meter

Figure 4. digital multi-meterFluke 179

Base plate was made of pure aluminum by smelting and casting, which contains a high thermal conductivity, base-plate dimensions of 205 mm length, 187 *mm* wide and 29 *mm* height. There are eight rectangular openings range from 6.5 *mm* to 15 mm and of different lengths (35 and 60 *mm*) are placed in the underside of the base plate. It is used to include the eight thermocouples are distributed on a base plate to measure the temperature of the base plate.

The main objective of the heating unit is to provide a flow of heat through the bottom surface of the base plate of the fins, the heater is made of chrome and nickel resistance tap 3 *mm*, 0.15 *mm* thickness and the resistance is 2.99 ohm *per meter*, was wrapped in a uniform manner on the mica plate (dielectric) 2-*mm* pitch, Upper and lower surfaces of the heater is covered with mica plate thickness of 0.8 *mm*. The heating unit fixed with the bottom surface of the base plate of small nails to hold good communication between the two sides. And input electric power to the heater was controlled by the self-adapter (varic) for a continuous flow of heat along the base of the painting, which is measured using a digital wattmeter.

On both sides of a hot plate was isolated by glass wool, 4.3 *cm* thickness and foam thickness of 4 *cm*. *Table 2* shows the thermal conductivity of insulation material.

Table. 2 Thermal conductivity of insulation materials.

Insulation material	Thermal conductivity K (W/m.k)
Calcium silicate (Gypsum)	0.17
Glass wool	0.04
Foamed	0.031
Ply wood	0.12
Hard wood	0.16

A set of thermocouples located be inserted at various points to measure the losses from the bottom surface of the heater. And there is another group of thermocouples were located in different locations to measure the loss of heat from the sides of the base plate.

Two screws installation placed at the other side of a wooden frame to rotate the model test in a corner of the tendency towards axis (normal to paper). To control the angle of inclination (β), was modified by protractor was fixed on the side of a wooden frame and the cursor is fixed on the wooden frame. Description Inclination is shown in *Figure 5.*

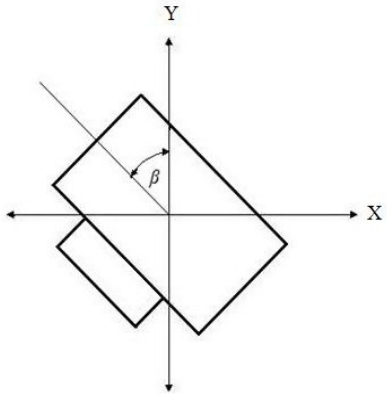

Figure 5.Schematic illustration of the angle of inclination of the model test.

Test fins are made of pure aluminum with the surface of highly polished to reduce the thermal radiation. The type of fin is rectangular with (t) thickness, (H) High, (L) and long. Dimensions of this topic are changed by doing experiments, and the fin thickness (t) is 6.5 *mm* and the length of the fins (L) was 187 *mm*. Fins were glued vertically upwards to the upper surface of the base plate and then rotated in horizontal position.

Figure 6. Experimental Set-up of Fin Array.

Taken into account when you paste the fins to be a glue layer [epoxy (k = 0.758 w/m.k)] is very thin so as to reduce the resistance to heat transfer from the base plate to a minimum, in addition to that notes the fact that the glue itself is connected to a good article. Fins are distributed along the upper surface of the base plate in different places; fin spacing S (the distance between the centers of two neighboring fins).And *Figure 6.* shows a picture of the Testing device.[8]

3. DATA REDUCTION

In the present study, the thermo physical properties in the Nu and Ra are evaluated at the film temperature, i.e.

$$T_f = \frac{1}{2}(T_b - T_\infty) \quad (1)$$

The average heat transfer coefficient can be calculated from the following relation:

$$h = \frac{Q_c}{A_t \eta_o (T_b - T_\infty)} \quad (2)$$

Where, (Q_c) is the convection heat transfer rate, (T_b) is the average temperature of the base plate, (T_∞) is the ambient air temperature, (η_o) is the overall fin efficiency and (A_{tot}) is the total surface area, to better calculate the heat transfer coefficient, one shall take into account the overall fin efficiency (η_o). The (η_o) for every test sample can be calculated and the lowest (η_o) encountered in the present study is around 0.99, so that (η_o) is reasonably assumed unity for simplicity.

The total heat generated from the heater (Q_t) is distributed into the heat transferred by convection to the quiescent air (Q_c) and the heat losses through the insulations to the surroundings (Q_{loss}).

$$Q_c = Q_t - Q_{loss} \quad (3)$$

Where,

$$Q_{loss} = Q_{cond} + Q_{rad} \quad (4)$$

Q_{cond} is the heat lost by conduction from the bottom side of the heater and sides of heat sink, and Q_{rad} is the heat transfer rate by radiation.

The radiation contribution (q_{rad}) can be estimated using the following equation [2]:

$$q_{12} = \frac{A_2 \sigma (T_1^4 - T_2^4)}{(A_2/A_1)[(1-\varepsilon_1)/(\varepsilon_1 A_1)] + 1} \quad (5)$$

The heat transfer rate by conduction can be calculated from the equation

$$q_{cond} = q_{bottom} + q_{edges} \quad (6)$$

Where, q_{bottom} is the heat lost by conduction from the bottom side of the heater. It is calculated from equation.

$$q_{bottom} = \frac{\Delta T}{\sum R_t} \quad (7)$$

Where ΔT is the overall temperature difference,$\sum R_{tot}$ is the total thermal resistance.

$$\sum R_t = \left(\frac{L_G}{K_G A} + \frac{L_W}{K_W A} + \frac{L_F}{K_F A} + \frac{L_P}{K_P A} + \frac{1}{h_o A}\right) \quad (8)$$

K is the thermal conductivity of insulation materials (as shown in table1), A is the area of the wall normal to the direction of heat transfer. L_G, L_W, L_F and L_P are the thickness of the insulation layers of Gypsum, glass wool, foamed and ply wood respectively in (y) direction and ho is the convection heat transfer coefficient to surroundings.

Also, heat lost by conduction from four sides of the base plate q_{edges}can be estimated from equation (7).By subtracting the conduction and radiation contribution, the heat transferred by natural convection can be determined.

4. UNCERTAINTY ANALYSIS

The experimental uncertainty is estimated using the uncertainty propagation equation proposed by J.P. Holman[21]. The percentage relative uncertainty in the measuring of the base plate temperature is 0.5208 %. The percentage relative uncertainty in the measured electric power input to the heater is 0.6%. the percentage relative uncertainty in measuring the orientation angle is 0.44 %. the percentage relative uncertainty in measuring the ambient air temperature is 1.66667%. The uncertainty in compound variables were found to be 0.60063 % for average heat transfer coefficient and average Nusselt number and 0.0264567 % for Rayleigh number.

5. NUMERICAL SOLUTION

5.1. PHYSICAL DOMAIN

A numerical solution was obtained with the CFD code. In principle, the code solves the governing set of elliptic partial differential equations for conservation of mass, momentum and energy. The buoyancy forces representation is based on the Boussinesq approximation. The flow is, therefore, considered as essentially incompressible. The fluid properties are assumed constant and are evaluated at the average of the hot surface and the ambient fluid temperatures. The solution is for conditions of steady stat laminar free convection ($Ra < 10^9$).

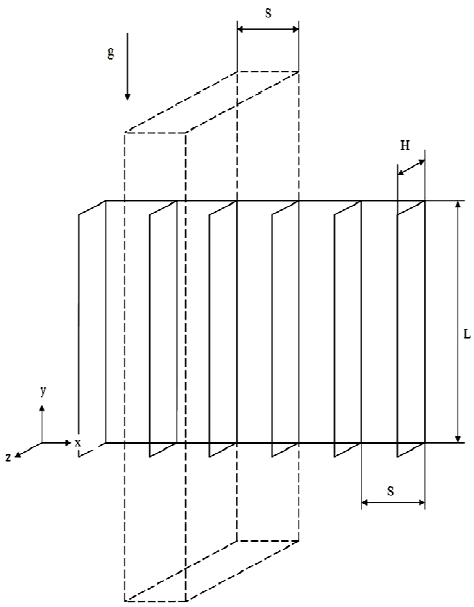

Figure 7. Schematic drawing of the fin array under investigation.

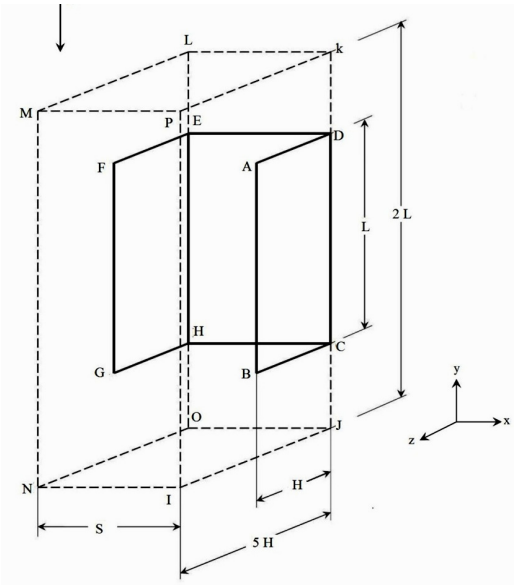

Figure 8. Schematic drawing of the computational domain with locations of the applied boundary conditions.

A schematic drawing of the fin array under investigation is shown in *Figure 7*.together with the actual simulated part of one fin. An infinite number of fins with negligible thickness was assumed. The fin surfaces and fin array base were assumed to be at a uniform temperature. The computational domain for the present problem is shown in *Figure 8* an infinite number of fins with negligible thickness were assumed.

The simulated part is shown in *Figure 8* in more detail. The computational domain has been beyond the actual dimensions of the fin array in order to account for effects due to surrounding of the fin array. Computations were performed for fin of L, H being the height of the fin, and S is (spacing) width of the domain in x-direction. The domain length was 2L in the x- direction and the height of the domain 5H in z-direction. The present study investigates the effects of a wide range of geometrical parameters to the heat transfer from fin arrays. Effects due to change in fin height, fin spacing, orientation angle and temperature difference between fin and surrounding are investigated.[8]

5.2. GOVERNING EQUATIONS

The natural convection flow under investigation was modeled by a set of elliptic partial differential equations describing the conservation of mass, momentum and energy in three rectangular Cartesian coordinate directions.

5.2.1 GOVERNING EQUATIONS FOR AIR

• Continuity:

$$\frac{\partial(\rho u)}{\partial x}+\frac{\partial(\rho v)}{\partial y}+\frac{\partial(\rho w)}{\partial z}=0 \qquad (9)$$

• Momentum equations in *x, y, z* directions are:

$$\frac{\partial(\rho u^2)}{\partial x}+\frac{\partial(\rho uv)}{\partial y}+\frac{\partial(\rho uw)}{\partial z}=-\frac{\partial(P_m)}{\partial x}+\rho v\left(\frac{\partial^2 u}{\partial x^2}+\frac{\partial^2 u}{\partial y^2}+\frac{\partial^2 u}{\partial z^2}\right) \quad (10)$$

$$\frac{\partial(\rho vu)}{\partial x}+\frac{\partial(\rho v^2)}{\partial y}+\frac{\partial(\rho vw)}{\partial z}=\frac{\partial(P_m)}{\partial y}+\rho v\left(\frac{\partial^2 v}{\partial x^2}+\frac{\partial^2 v}{\partial y^2}+\frac{\partial^2 v}{\partial z^2}\right)+g(\rho-\rho_\infty) \quad (11)$$

$$\frac{\partial(\rho wu)}{\partial x}+\frac{\partial(\rho wv)}{\partial y}+\frac{\partial(\rho w^2)}{\partial z}=-\frac{\partial(P_m)}{\partial z}+\rho v\left(\frac{\partial^2 w}{\partial x^2}+\frac{\partial^2 w}{\partial y^2}+\frac{\partial^2 w}{\partial z^2}\right) \quad (12)$$

• Energy equation:

$$\frac{\partial(\rho uT)}{\partial x}+\frac{\partial(\rho vT)}{\partial y}+\frac{\partial(\rho wT)}{\partial z}=\frac{v}{P_r}+\rho v\left(\frac{\partial^2 T}{\partial x^2}+\frac{\partial^2 T}{\partial y^2}+\frac{\partial^2 T}{\partial z^2}\right) \quad (13)$$

5.2.1 GOVERNING EQUATIONS FOR FIN

$$\left(\frac{\partial^2 T}{\partial x^2}+\frac{\partial^2 T}{\partial y^2}+\frac{\partial^2 T}{\partial z^2}\right) \quad (14)$$

In the above equations it is apparent that the Boussinesq approximation has not been applied. The assumptions employed in the governing equations are in agreement with steady, incompressible, laminar flow of air with constant properties, except for density which is taken as a function of temperature only, $\rho = \rho(T)$. Radiation heat loss is neglected. The buoyancy forces representation is based on the Boussinesq approximation.[8]

5.3. BOUNDARY CONDITIONS

In a numerical simulation, it is impossible and unnecessary to simulate the whole universe. Generally we choose a region of interest in which we conduct a simulation. The interesting region has a certain boundary with the surrounding environment. Numerical simulations also have to consider the physical processes in the boundary region. In most cases, the boundary conditions are very important for the simulation region's physical processes. Different boundary conditions may cause quite different simulation results. Improper sets of boundary conditions may introduce nonphysical influences on the simulation system, while a proper setof boundary conditions can avoid that. So arranging the boundary conditions for different problems becomes very important.

All boundary conditions were implemented by the inclusion of additional source and /or sink terms in the finite volume equations for computational cells at the boundaries. In natural convection flows there is no information regarding the velocity temperature fields before the start of calculations. Since governing, equations are invariably coupled, the temperature field causes the velocity field to develop and in turn the velocity field affects the temperature field with the promotion of convective heat transfer. The imposed boundary conditions were as follows [8]:

1. The fin surface (ABCDA and EFGHE) and base surface (CDEHC) were held at. constant temperature.
2. Symmetry boundary conditions were applied at surface IJCDKPI, PKLMP, MNOHELM and IJONI.

3. No-slip boundary conditions were applied to fin walls to simulate the effect of laminar friction and heat transfer.
4. All the remaining surface were open surfaces where air enters and leaves the surface at the ambient temperature T_∞ and the corresponding density T_∞Here the ambient pressure was used as a stagnation boundary condition with the incoming mass having T_∞.

5.4. COMPUTATIONAL PROCEDURE

In this study, a numerical investigation has been carried out to reveal the mechanism of fluid flow and heat transfer from a vertical rectangular fin attached to a partially heated horizontal base. The problem is a conjugate conduction-convection heat transfer problem with open boundaries. The governing equations for the problem are the conservation of mass, momentum and energy equations for the fluid and the heat conduction equation for the fin. The control volume technique based on the ***simplex*** algorithm with a non staggered grid arrangement is employed to solve the governing equations. The effect of the heated base, on the mechanism of the fluid flow and heat transfer, is numerically investigated. Temperature distribution and flow patterns around the fin are plotted to support the discussion. Results are obtained for air at laminar and steady flow.

The system of *Equations [(9)-(14)]* with the boundary conditions stated above is solved through a control volume to obtain a set of discretized linear algebraic equations.These equations were solved by the widely used commercial CFD package FLUENT 6 employing the SIMPLEST algorithm for the pressure correlation processalong with the solution procedure for the hydrodynamic equations. The central-difference-scheme leads to a second order truncation error in the approximations, whereas the upwind-scheme gives only first-order accuracy. The discretized equations are solved by the TDMA (Tri Diagonal Matrix-Algorithm).

6. EXPERIMENTAL RESULTS

6.1. EFFECT OF TEMPERATURE DIFFERENCE

As a point of departure for the presentation of convective heat transfer coefficient (h) , from fin arrays are plotted to ambient temperature difference $(T_F – T_\infty)$ at different values of orientation angle (Φ) and fin height (H).

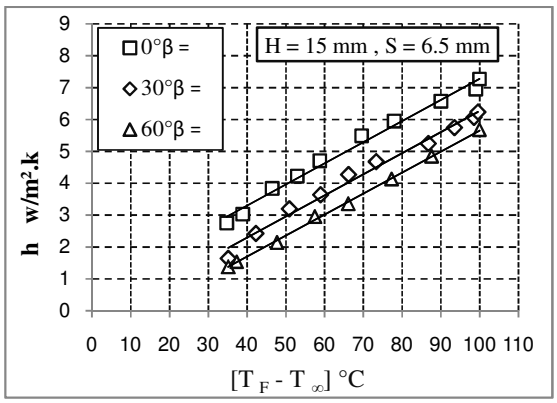

Figure9. Variation of heat transfer coefficient with temperature difference T

at H = 15 mm S = 6.5 mm.

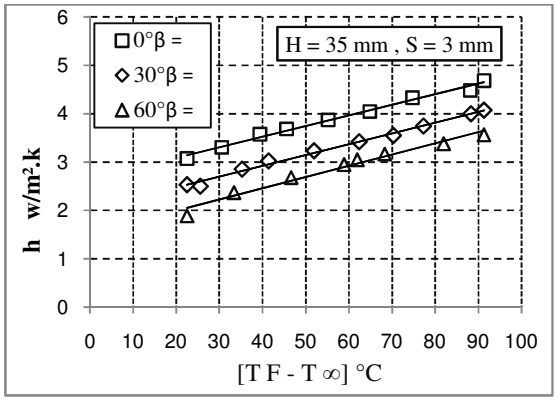

Figure 10. Variation of heat transfer coefficient with temperature difference T at H = 35 mm S = 3 mm.

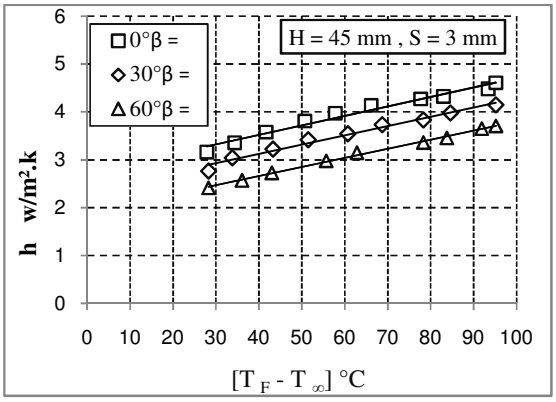

Figure11. Variation of heat transfer coefficient with temperature difference T at H = 45 mm S = 3 mm.

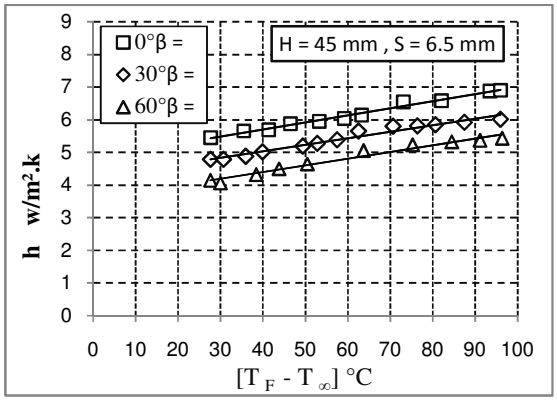

Figure 12. Variation of heat transfer coefficient with temperature difference T at H = 45 mm S = 6.5 mm.

The samples of these plots are given in *Figures [(9) - (12)]* the results for the fin heights of H = 15 *mm*, H=35 *mm* and H = 45 the fin spacing is s = 3 *mm*, s=6.5 *mm* and s = 16 *mm*, and the fin lengths are L =187 *mm*. These figures reveal that convection heat transfer rate from fin arrays is dependent on fin height, fin length and base-to ambient temperature difference. Essentially, fin heat transfer rate increases with fin height, fin length and base-to - ambient temperature difference. At low temperature differences, heat transfer rates are closer to each other and tend to diverge at higher temperature differences. Moreover, with larger fin heights, the increase of convection heat transfer rate with temperature difference is sharper For all fin arrays.

6.2. EFFECT OF FIN SPACING

To see the effect of base-to-ambient temperature difference more clearly. In *Figures [(13),(14)]*, convection heat transfer rates are plotted as a function of fin spacing. show the effect of fin spacing on heat transfer rate per unit base area at various orientation angle and fin spacing. It is seen that the heat-transfer rate per unit base area increases with increasing the fin spacing to each a maximum value and then decreases with farther increase in the fin spacing. On each curve, clearly, the maximum volumetric heat dissipation occurs at optimal spacing S_{opt} = 6.5 *mm.*

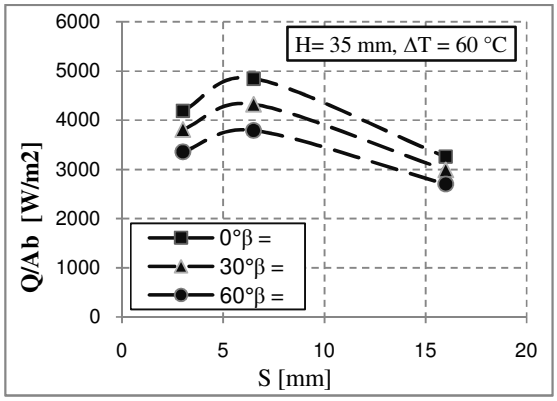

Figure 13. Variation of Convection Heat Transfer Rate with Fin Spacing, at different values of orientation angles (H = 35, Δ T = 60°C).

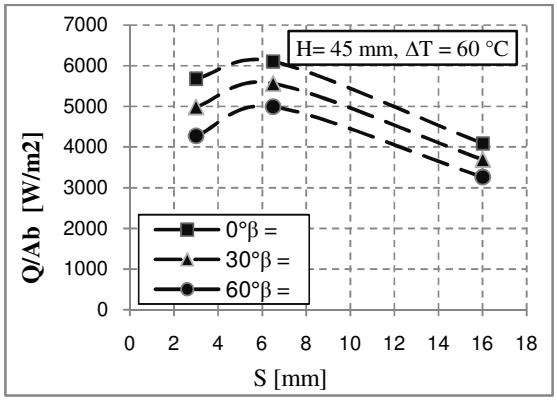

Figure14. Variation of Convection Heat Transfer Rate with Fin Spacing, at different values of orientation angles (H = 45, Δ T = 60°C).

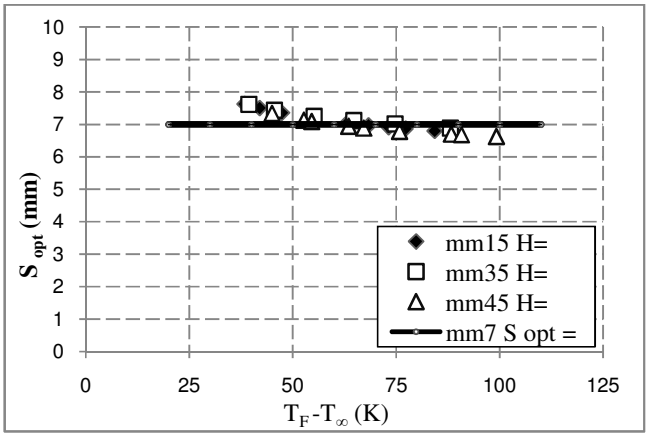

Figure 15. Optimum fin spacing's as a function of fin height and base-to-ambient temperature difference

Convection heat transfer rate is maximized is called optimum fin spacing, S_{opt}. Closer inspection of these figures reveals that optimum fin spacing depends on fin height and base-to-ambient temperature difference.*Figure 15*displays the optimum fin spacing's as a function of fin height and base-to-ambient temperature difference. As seen from this figure, optimum fin spacing doesn't vary significantly with neither fin height nor base-to-ambient temperature difference. Therefore, for practical purposes, the optimum fin spacing to maximize the convection heat transfer rate may be taken as 7 *mm* for arrays with fin heights from 15 to 45 *mm* and fin length 187 *mm*, for base-to-ambient temperature differences from 30 to 100 K.

6.3. EFFECT OF FIN HEIGHT

For all the cases the heat transfer rate increases with the increase in the temperature difference. In addition, the increase rates are also similar. *Figures [(16)-(18)],* show variation of heat transfer rate per unit base area (Q/A_b) with fin height (H), at various orientation angles (β) and different values of fin spacing (S).

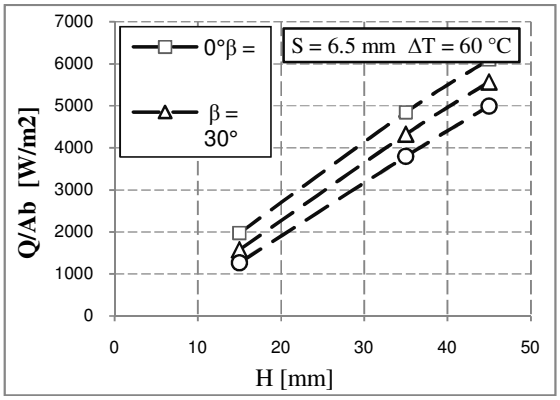

Figure 17. Variation of heat transfer rate per unit base area with fin height at various β (S = 6.5 mm, ΔT = 60°C).

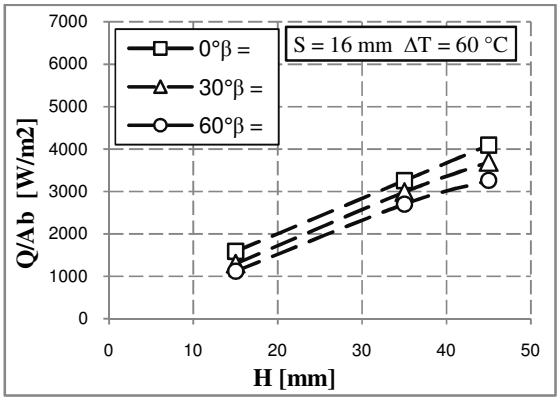

Figure 18. Variation of heat transfer rate per unit base area with fin height at various β (S = 16 mm, ΔT = 60°C).

These Figures show that the-heat transfer per unit base area increases with increase in fin height (H) for all values of orientation angle and fin spacing. The reason is that, any increase of fin height increases the array surface area and thereby entails a larger heat transfer rate.

6.4. EFFECT OF ORIENTATION ANGLE

Effects of orientation angle (β) on the heat transfer coefficient are shown in *Figures. [(19),(20)]*. These Figures are presented at different values of fin spacing. It is seen from the figures that the average heat transfer coefficient has a maximum value at β = 0° and reduce with the increase in (β) to reaches a minimum value at β = $60^0$and thus increase with farther increase in β.

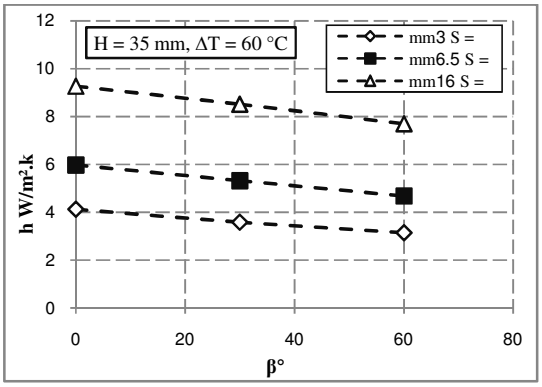

Figure 19. The dependence of heat transfer coefficient h on the orientation angles at various fin spacing H = 35 mm, ΔT = 60 °C.

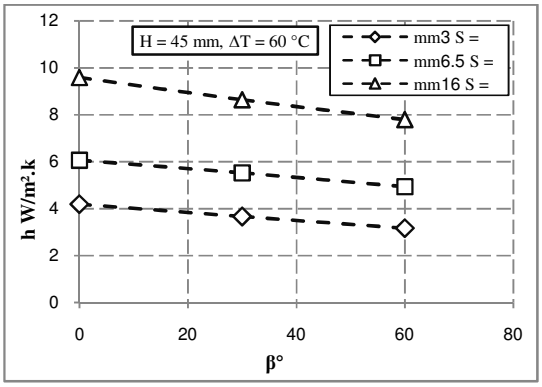

Figure20. The dependence of heat transfer coefficient h on the orientation angles at various fin spacing H = 45 mm, ΔT = 60 °C.

*Figures*show that the heat transfer coefficient increases with increase in fin spacing. These figures show also a variation of heat transfer coefficient with orientation angle (β) at various fin height. It is seen that, the heat transfer coefficient has a maximum values at β = 0°, while has a minimum values at β = 60^0 for all values of H. Inspection of the influence of the fin height on the averaged heat transfer coefficient indicates that it is quite small.

6.5. EFFECTS OF VARIATIONS IN FIN HEIGHT

Effects of variations in fin height on the heat transfer coefficient are shown in *Figure (21),* for various fin spacing's and fin lengths. On the overall, the heat transfer coefficient values do increase with increase in the fin height.

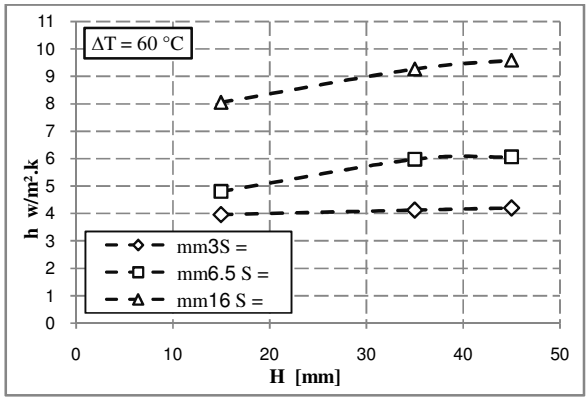

Figure21. Effects of variations in fin height on the heat transfer coefficient for different fin length and fin spacing values.

Although a small drop with increase in the fin height, specially for the smallest fin spacing, so the increase in convective heat transfer rate with fin height is not significant. However, one can see that it is very difficult to draw clear conclusions due to the various parameters involved.

Figures [(22) - (23)] presents overall Nusselt numbers for a range of Rayleigh numbers. Various cases are presented where fin height and fin length were changed. As can be seen from the data points plotted from the present simulations, the differences between the various cases are very small for high Ra numbers, but somehow more distinct for smaller Ra numbers.

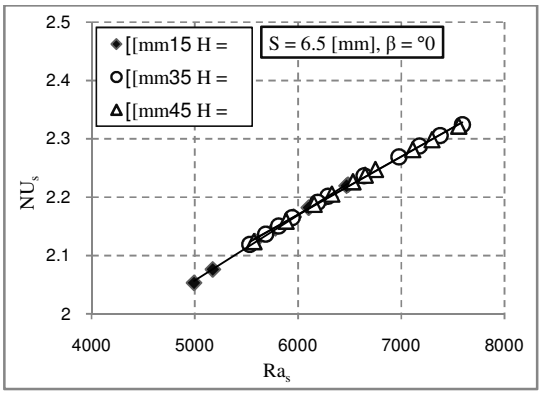

Figure24. Variation of Nusselt number Nu_s with Rayleigh number Ra_sat S = 6.5 mm.

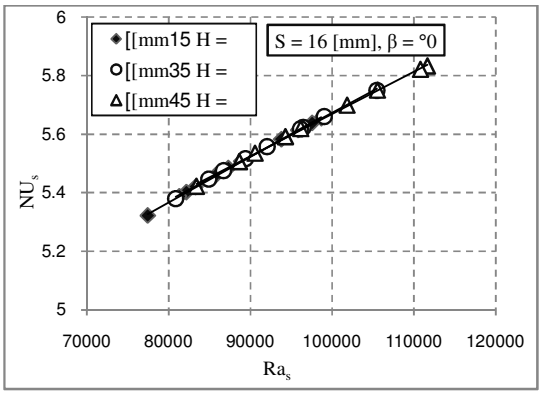

Figure25. Variation of Nusselt number Nu_s with Rayleigh number Ra_sat S = 16 mm.

In order to compare present results with data from the literature a best fit line for all the numerical results was obtained.to confirm the method of calibration, a vertical fins was mounted onto the set-up and the Nusselt numbers were determined both experimentally and by using various correlations from literature. The vertical plat was heated at steady state, the temperature of the vertical plate, T_F the ambient temperature, T_∞ and the power input were measured. The output heat transfer rate from the plate was determined.

Rayleigh number was defined as,

$$Ra = \frac{g.\beta.(T_F - T_\infty).S^3}{\nu.\alpha} \quad (15)$$

where S, the spacing between fins. The physical properties necessary to evaluate Rayleigh and Nusselt numbers were taken at film temperature,$T_{film} = (T_F + T_\infty)/2$. The heat transfer coefficient based on the area of the vertical plate and thus the Nusselt number were evaluated as,

$$h_{exp} = \frac{Q_{tot}}{A.(T_F - T_\infty)} \quad (16)$$

$$Nu = \frac{h_{exp}.S}{k} \quad (17)$$

After the determination of the experimental Nusselt numbers, several correlations from literature were utilized to evaluate and compare the Nusselt numbers. The correlations chosen are,Churchill and Chu's first relation (for laminar and turbulent flows) [13]:

$$Nu_{th1} = \left[0.825 + \frac{0.378 \times (Ra)^{1/6}}{\left[1 + \left(\frac{0.492}{Pr}\right)^{9/16}\right]^{8/27}}\right]^2 \quad (18)$$

For $10^{-1} < Ra < 10^{12}$

Churchill and Chu's second relation (for Laminar flow only) [13]:

$$Nu_{th2} = 0.68 + \frac{0.670 \times (Ra)^{1/4}}{\left[1 + \left(\frac{0.492}{Pr}\right)^{9/16}\right]^{4/9}} \quad (19)$$

For $10^{-1} < Ra < 10^{9}$

McAdams' relation [13]:

$Nu_{th3} = 0.59 . (Ra)^{1/4}$ $10^4 < Ra < 10^9$ (20)

Churchill and Usagi's relation [13]:

$$Nu_{th4} = \frac{0.670 . (Ra)^{1/4}}{\left[1 + \left(\frac{0.492}{Pr}\right)^{9/16}\right]^{4/9}} \quad (21)$$

For$10^5 < Ra < 10^9$

The above correlations were also plotted, along with the experimental data, as displayed in *Figures [(27), (30)]*. These results reveal that except for the McAdams' correlation, which is a very rough correlation, the experimental data are in excellent agreement with the results from literature. For McAdams' correlation, the average relative error is 3.485 % while for the others it is less than 3 %. This agreement confirms the validity of the experimental set-up, the experimental procedure and the calibration procedure.[13]

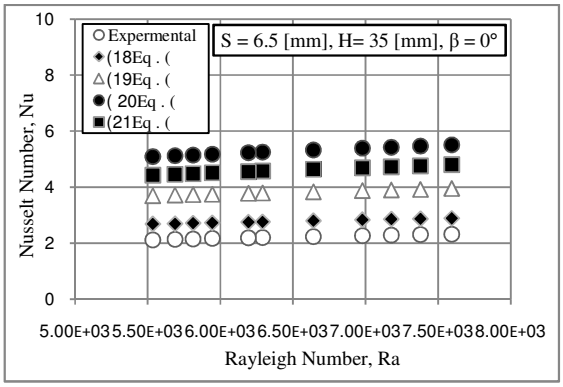

Figure 27. Comparison of experimental Nusselt number with correlation from literature at S = 6.5 mm and H = 35 mm

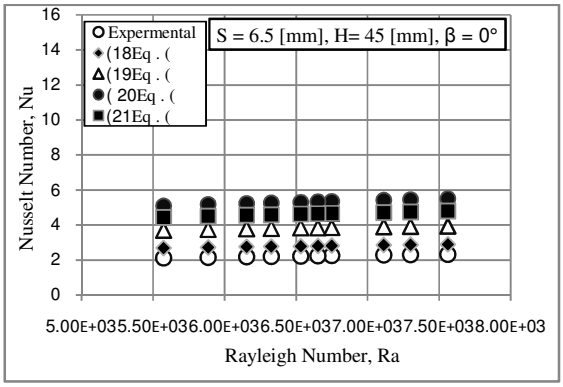

Figure 29. Comparison of experimental Nusselt number with correlation from literature at S = 6.5 mm and H = 45 mm

6.6. EFFECT OF FIN EFFICIENCY

In contrast to the fin efficiency η_f. which characterizes the performance of a single fin. the overall surface efficiency η_o characterizes an array of fins and the base surface to which they are attached. Representative arrays, where S designates the fin pitch, the total surface area is

$$A_t = NA_f + A_b \tag{22}$$

The maximum possible heat rate would result if the entire fin surface. as well as the exposed base, were maintained at T_b.

Recalling the definition of the fin thermal resistancethat is,

$$R_{t,c} = \frac{L}{kA} \tag{23}$$

$$R''_{t,c} = \frac{L}{k} \tag{24}$$

where $R_{t,o}$is an effective resistance that accounts for parallel heat flow paths by conduction/convection in the fins and by convection from the prime surface.

The fins are machined as an integral part of the wall from which they extend, there is no contact resistance at their base. However, more commonly, fins are manufactured separately and are attached to the wall by adhesive joint. Alternatively, the attachment may involve a press fit, for which the fins are forced into slots machined on the wall material, there is a thermal contact resistance, $R_{t,c}$ which may adversely influence overall thermal performance. An effective circuit resistance may again be obtained, where, overall surface efficiency is

$$\eta_{o(c)} = 1 - \frac{NA_f}{A_t}\left(1 - \frac{\eta_f}{C_1}\right) \tag{25}$$

Where,

$$C_1 = 1 + \eta_f hA_f\left(R''_{t,c}/A_{c,b}\right) \tag{26}$$

The efficiency $\eta_f$depends on the fin spacing; if the heat flux from the fin tip is negligible the following expression for $\eta_f$can be used:

$$\eta_f = \frac{tanh\, mL_c}{mL_c} \tag{27}$$

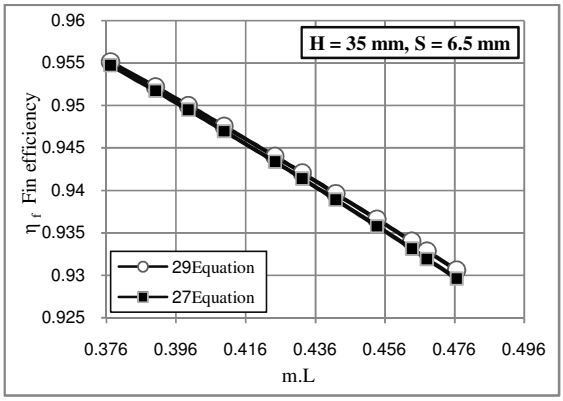

Figure 31. Values of fin efficiency η calculated by Eq.(6.13). and simplified relation from ref (22) Eq. (6.15). shown as the group mL at S = 6.5 mm and H =35 mm

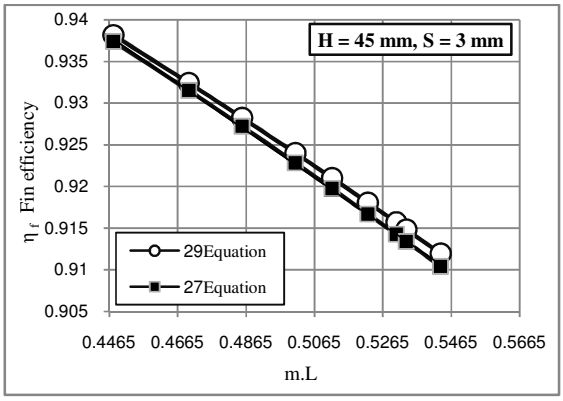

Figure32. Values of fin efficiency η calculated by Eq.(24). and simplified relation from ref (22) Eq. (26). shown as the group mL at S = 3 mm and H =45 mm

Where the width of a rectangular fin is much larger than its thickness, w ≫ t, the perimeter will be approximated as P = 2w, and the group mL can be written as

$$mL_c = \left(\frac{hP}{kA_c}\right)^{1/2} L_c = \left(\frac{2h}{kt}\right)^{1/2} L_c \qquad (28)$$

when the product mL is not larger than unity, the fin efficiency can be approximated by the following relation:

$$\eta = \frac{1}{\left[1 + \frac{1}{3}(mL)^2\right]} \qquad mL \leq 1 \qquad (29)$$

In *figures [(31), (32)]* are shown the (η) values calculated from (24) and (26); it is apparent that (26) is a good approximation for η for mL ≤ 1.

6.4 EFFECT OF CONVECTIVE HEAT TRANSFER RATE

The convective heat transfer rates from fin arrays are plotted as a function of base-to-ambient temperature difference for fin spacing, s = 3, 6.5, 16 *mm* and for fin length, L = 187 and *Figs.[(33)-(36)],* respectively.

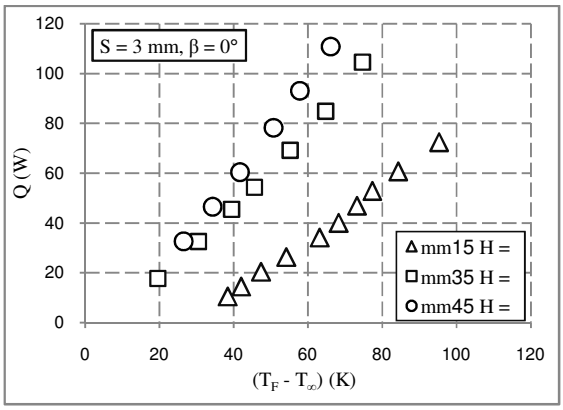

Figure33. Variation of convective heat transfer rate with fin height at a fin spacing of s = 3 mm and at a fin length of L = 187 mm

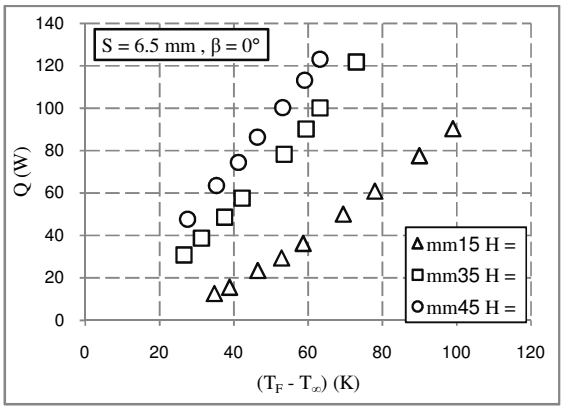

Figure34. Variation of convective heat transfer rate with fin height at a fin spacing of s = 6.5 mm and at a fin length of L = 187 mm

Eachof the figures involves the results, plotted for three finheights H = 15, 35 and 45 *mm*. For all fin arrays,these figures show that, the convective heat transfer rate from fin arrays depends on fin height, fin length,fin spacing and base-to ambient temperature difference.The convective heat transfer rates from the finarrays increases with fin height, fin spacing to ambienttemperature difference. The curves in thesefigures show similar trends for identically spaced finarrays. The convective heat transfer rates measuredfrom three different fin heights.

The heat transfer rate increases monotonously with temperature difference between fin base and surroundings, $T_F - T_\infty$. However, in fin arrays with small fin height the rate of increase of heat transfer rate with temperature difference is smaller than those ones with large fin height.

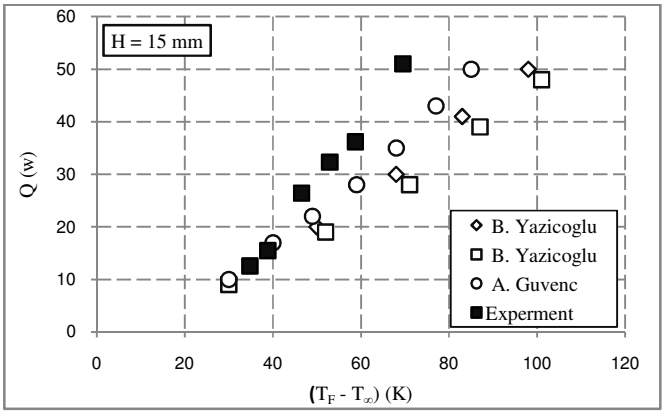

Figure 36. Comparison of the variation of the heat transfer rate with the temperature for the Experimental work with Similar projects from Ref. [13, 15].

NUMERICAL RESULTS

Height, orientation angel and temperature difference between fin and surroundings on the free convection heat transfer from horizontal fin arrays was carried out. The three-dimensional elliptic governing equations were solved using a finite volume based computational fluid dynamics (CFD) code. Preliminary simulations were made for cases reported in the literature. After obtaining a good agreement with results from the literature a large number of runs were performed for a detailed parametric study. It has been shown that it is not possible to obtain optimum performance in terms of overall heat transfer by only concentrating on one or two parameters. The interactions among all the design parameters must be considered. Results are presented in graphical form together with optimum values and correlations, and compared with available experimental data from the literature.

It is important to understand the general flow patterns dominating flows from fin arrays. In natural convection flows there is no information regarding the velocity and temperature field, the temperature field cases the velocity field to develop and turn the velocity field affects the temperature field with the promotion of convection heat transfer. *Figures [(37), (38)]* show streamline and heat flux contours for orientation angle $\beta = 0°$.

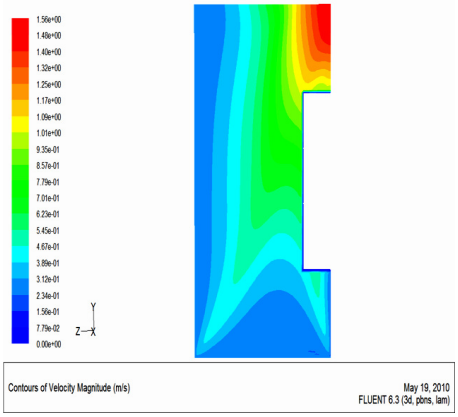

Figure37. Streamline contours at S=6.5 mm, H= 45 mm, β= 0°

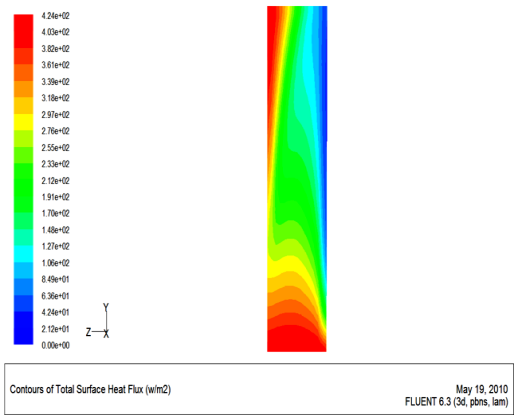

Figure 38. contours of total surface heat flux at S=6.5 mm, H= 45 mm, β= 0°

Effect of temperature difference ΔT on average heat transfer coefficient at various orientation angle and different values of fin spacing S, fin height H are shown in figures [(39) - (41)]. Also, it is seen that the average heat transfer coefficient increases with increasing ΔT for all values of orientation angle β. It is clear also; the-heat transfer coefficient increases With decreasing orientation angle.

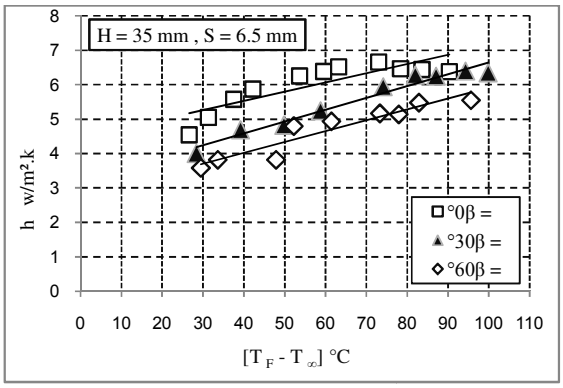

Figure 40. Variation of heat transfer coefficient with temperature difference ΔT at H= 35 mm, S = 6.5 mm.

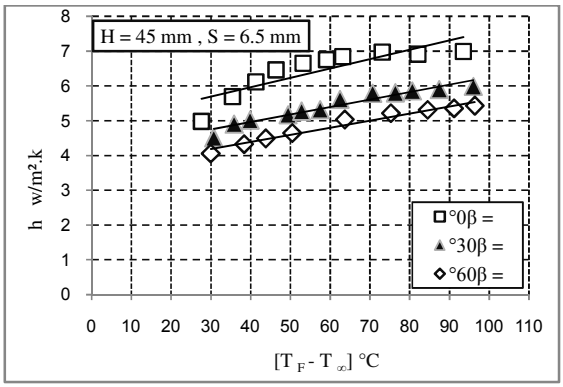

Figure 41. Variation of heat transfer coefficient with temperature difference ΔT at H= 45 mm, S = 6.5 mm.

Figure 42. indicates the variation of heat flux along the fin length. From this distribution it is clear that the rate of heat dissipation from the central portion is less.

This justifies where single chimney flow pattern is present, a stagnant zone is created at the central bottom portion of fin array channel and hence it does not contribute much in heat dissipation.

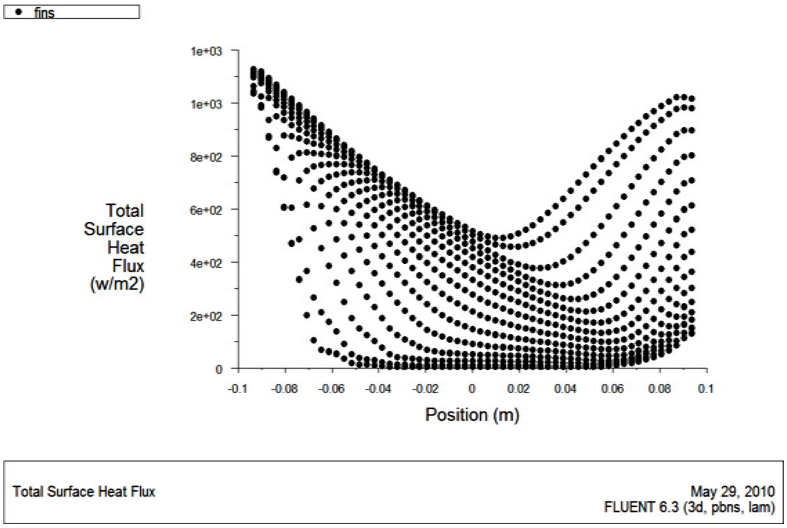

Figure42. Variation of Heat Flux along Fin Length

Comparisons between experimental and numerical results are presented in Figures[(43)-(45)]From these figures, it is that a good agreement between experimental and numerical results with a maximum deviation of 0.905220036 %. Table 3 shows a deviation of the experimental results from numerical results at S = 6.5 mm, ΔT = 35°C to 95°C.

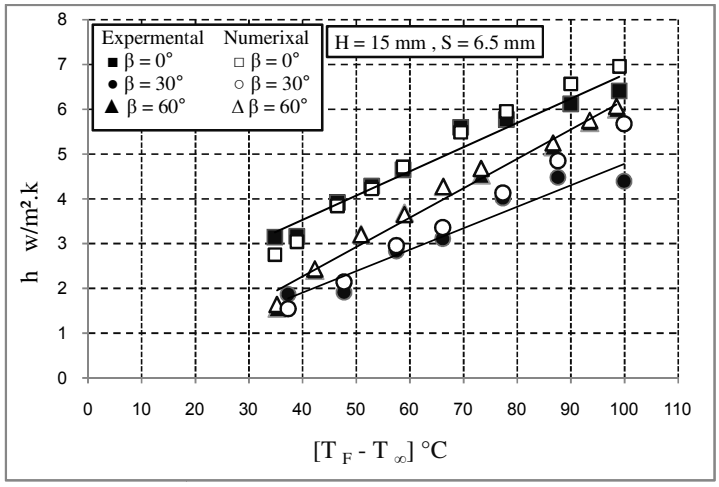

Figure43. Validation of the computational-approach: present study CFD results compared with experimental dataat H = 15 mm.

Table 3. Deviation of the CFD prediction from experimental results.

Orientation angle β	H = 15 mm	H = 35 mm	H = 45 mm
β = 0°	0.113734849	0.145819165	0.58455242
β = 30°	0.111104765	0.003567939	0.053878139
β = 60°	0.905220036	0.173563504	0.010789964

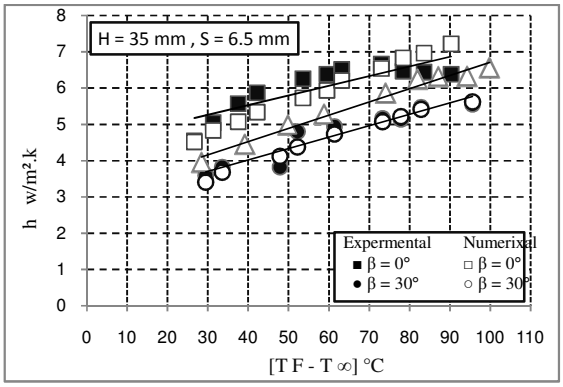

Figure44. Validation of the computational-approach: present study CFD results compared with experimental data at H =35 mm.

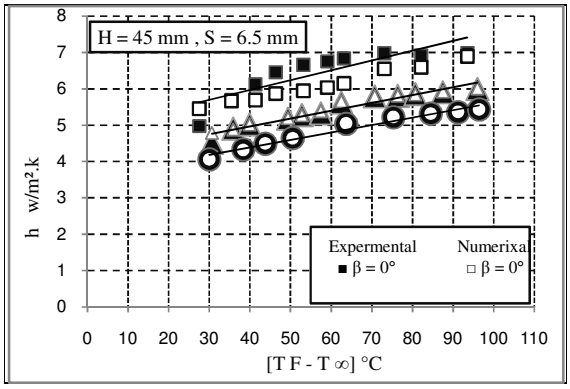

Figure45. Validation of the computational-approach: present study CFD results compared with experimental data at H = 45 mm.

6.7. EMPIRICAL EQUATIONS

A correlation for average Nusselt number has been presented to relate the heat transfer from fin arrays in channel with dimensionless, Rayleigh number, modified experimental parameters such as fin spacing, fin height, fin length and orientation angle.

Four empirical equations are derived to correlate the mean Nusselt number as a function of Rayleigh number, fin spacing ratio, fin height ratio , and orientation angle as follows:

$$Nu_L = 50.08 \left[Ra_L \frac{(S)}{H}\right]^{-6.8229E-05} \left(\frac{L}{H}\right)^{1.04E-07} \left(\frac{L}{S}\right)^{5.12E-10} Cos\beta^{1.1E-06} \qquad (30)$$

These equation are valid for tested finned model with thickness t = 6.5 mm, fin height H = 15 to 45 mm, and fin spacing S = 3 to 16 mm, Rayleigh number ranged from $1.19x10^8$ to $1.87xl0^8$ and at constant fin length L, with relative error = ± 15.3474 %.

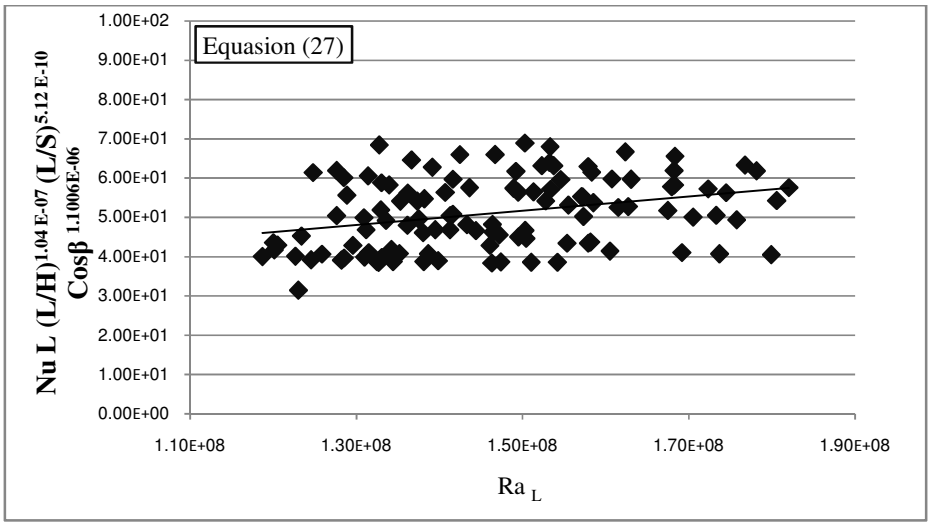

Figure46.Correlation obtained from the present study.

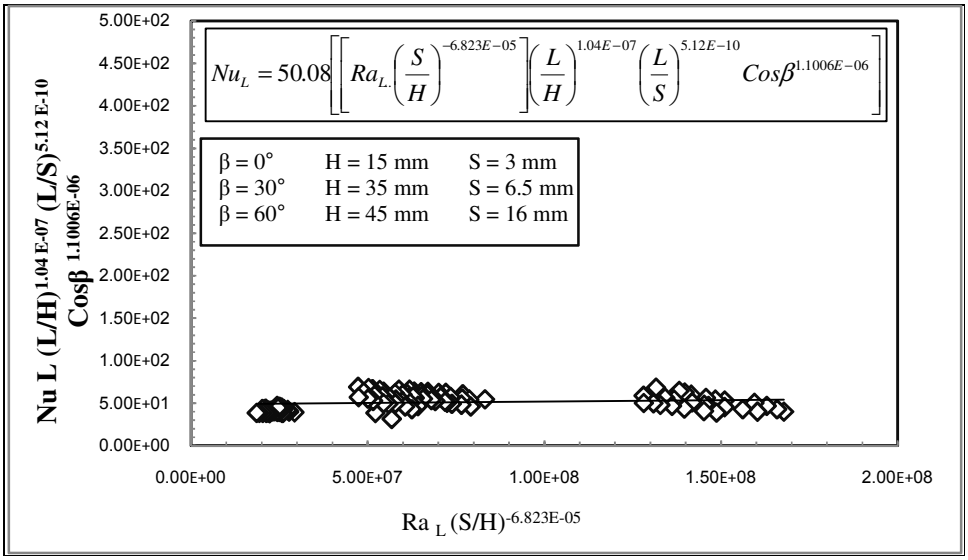

Figure 47. Result of generalizing data of the present work relying on the non-dimensional parameters

The reader should note that this correlation is only valid for thin fins which do not cause much effect on longitudinal air flow. And this correlation does not show effects of fin cross sectional area, thermal conductivity and heat transfer coefficient of the fin.

CONCLUSIONS

This work presents experimental results of heat transfer by free convection from rectangular fins on a vertical base. From the experimental results, it can be concluded that the geometric parameters of fin array, fin height, fin length and fin spacing and base-to-ambient temperature difference affects the rate of convection heat transfer primarily. The separate roles of these parameters and base-to-ambient temperature difference, and numerical investigations have been performed to study the natural convection heat transfer from a rectangular fin arrays at different orientation angles.

From the results plotted in the figures, it can be seen

- the average heat transfer coefficient has a maximum value at β = 0°. It decreases with the increase of (β)to reach a minimum value at β = 60°. This is due to that at β = 0°
- the larger fin height results in higher convection heat transfer rate from the fin arrays. Although, at low base-to-ambient temperature differences, the increase in convective heat transfer rate with fin height is not significant.
- at higher temperature differences the convective heat transfer rate increases significantly with fin height.
- For a given base-to ambient temperature difference, the increase in heat transfer rate with fin height is steeper for smaller fin spacing. Since, the fin array with smaller fin spacing has higher fin number.
- the increase in fin height causes larger heat transfer area and higher convection heat transfer rate.

- the heat transfer rate per unit base area increases with the increase in the fin spacing to reach a maximum value and then decreases with farther increase in the fin spacing. the maximum heat dissipation occurs at optimal spacing $S_{opt} = 7\ mm$.
- Optimum fin spacing depends on fin height and base to-ambient temperature difference, but this dependence is not very strong. Thus, for practical reasons, the optimum value may be taken as 7 mm, for fin heights from 15 to 45 mm for fins of 187 mm length. These results are consistent with those of previous authors.
- the heat transfer coefficient values do increase with increase in the fin height. Although a small drop with increase in the fin height, specially for the smallest fin spacing, so the increase in convective heat transfer rate with fin height is not significant.
- As can be seen from the data points plotted from the present simulations, the differences between the various cases are very small for high Ra numbers, but somehow more distinct for smaller Ra numbers.
- The array length, fin spacing, and surface temperature mostly affect the heat transfer coefficient. The fin height does not affect much the heat transfer coefficient.
- Excellent agreement was obtained among the analytical, numerical and experimental results.
- Empirical correlations were derived to correlate the Nusselt number as a function of Rayleigh number, fin spacing ratio, fin height ratio, and orientation angle. The general empirical formulae obtained from the present study are given in the form:

$$Nu_L = 50.08\left[Ra_L\left(\frac{S}{H}\right)\right]^{-6.8229E-05}\left(\frac{L}{H}\right)^{1.04E-7}\left(\frac{L}{S}\right)^{5.12E-10} Cos^{1.1E-06}$$

at $\beta \leq °60 \mathrm{Ra_L} < 1\times 10^{10}$

REFERENCES:

[1] CengleYunus, Heat transfer: a practical approach, 2nd Ed.New York (2003).

[2] Incropera, F.P. and DeWitt, D.P., Introduction to heat transfer, John Wiley and sons, NY. (1996).

[3] BurakYazicioğlu,HafitYüncü, A Correlation For Optimum Fin Spacing Of Vertically-Based Rectangular Fin Arrays Subjected To Natural Convection Heat Transfer, Middle East Technical University, Department of Mechanical Engineering, (09. 03. 2009) pp 99-105.

[4] V. Dharma, S.V. Naidu, B. Govinda and K.V. Sharma, Combined Convection and Radiation Heat Transfer from a Fin Array with a Vertical Base and Horizontal Fins, PVG's College of Engineering and Technology, Andhra University, India, (October 24-26, 2007) pp 978-988-98671-6-4.

[5] R.L. Edlabadkar, N.K. Sane, G.V. Parishwad, Computational Analysis Of Natural Convection With Single V-Type Partition Plate, Pvg's College Of Engg. And Technology, Pune, IndiaJspm's College Of Engineering, Pune, India-411028. Gov College Of Engineering, Pune, India.

[6] Denpong, MasudBehnia, And David Copeland, A comparison of fin geometries for heat sinks in laminar forced convection, School of mechanical and manufacturing engineering , the university of newsSouth wales sydney 2052, Australia.(2001) pp 68-76.

[7] Arularasan R. And Velraj R. Assistant Professor, cfd analysis in a Heat sink for cooling of electronic devices, department of mechanical engineering, ssn college of engineering, tamilnadu, India. Vol. 16.No.3 (September-December, 2008) pp 1-11.

[8] A. Abdel-Latif, T. Abdel-Salam, H. Ashour, Orientation effect on natural convection performance of longitudinal fin arrays heat sink, mech. power eng.dept, zagazig university, faculty of engineering,, Egypt(30/06/2008) pp 283-296.

[9] SidyNdao, YoavPeles, Michael K. Jensen, Multi-objective thermal design optimization and comparative analysis of electronics cooling technologies, department of mechanical, aerospace, and nuclear engineering, rensselaer polytechnic institute, troy. (20 May 2009) pp 4318-4326.

[10] Seri Lee, Optimum design and selection of heat sinks, Aavid Engineering Inc. Laconia, New Hampshire. Pp 48-54

[11] Christopher L. Chapman., and Seri Lee, Thermal performance of an elliptical pin fin heat sink ,Aavid Engineering, Inc. Laconia, New Hampshire, California. pp 24-31.

[12] Rong-Hua, Shih-Pin Liaw and Ming Chang, Optimum spacing's of longitudinal convective fin arrays. Department of marine engineering and technology (1997) pp 47-53.

[13]. A. Guvenc, H. Yuncu, An experimental investigation on performance of fins on a horizontal base in free convection heat transfer, Department of Mechanical Engineering, Middle East Technical University,063150 Ankara Turkey (16 February 2000) pp 409-416.

[14]. F. Harahap, H. Lesmana, Measurements of heat dissipation from miniaturized vertical rectangular fin arrays under dominant natural convection conditions, Mechanical Engineering Department, Thermal Engineering Laboratory, Institute of Technology of Bandung , Indonesia, 42 (2006) pp 1025–1036.

[15]. B. Yazicioglu and H. Yuncu, Optimum fin spacing of rectangular fins on a vertical base in free convection heat transfer, Department of Mechanical Engineering, Middle East Technical University, Ankara 06531, Turkey, Heat Mass Transfer 44 (2007) pp 11–21.

[16]. Van de Pol, D.W., and Tierney, J.K. Free Convection Heat Transfer from Vertical Fin Arrays, IEEE Trans. Part, Hybrids, and Packaging, (1974).

[17] Bilitzky, A. The Effect Of Geometry On Heat Transfer By Free Convection From A Fin Array, MS Thesis, Dept. Of Mechanical Engineering, Ben-Gurion University Of The Negev, Beer Sheva, Israel, (1986).

[18] Kraus, A.D. and Bar-Cohen, A. Design And Analysis Of Heat Sinks, John Wiley And Sons, New York, (1995) pp. 305-320.

[19] Jones, C.D, and Smith, L.F. Optimum Arrangement Of Rectangular Fins On Horizontal Surfaces For Free Convection Heat Transfer, ASME Journal Of Heat Transfer, 92 (1970) pp 6-10.

[20] Harahap, F, and McManus, H.N. Natural Convection Heat Transfer From Horizontal Rectangular Fin Arrays, ASME Journal Of Heat Transfer, 89 (1967) pp. 32-38.

[21] J.P. Holman, Experimental Methods for Engineers, Publisher: McGraw-Hill Science/Engineering/Math, March 2, 2009.

[22] Andrea de lieto V , Stefano G , Franco G, Optimum design of vertical rectangular fin arrays, University of Rome ' Sapienza ' Department of fisicatecnica via eudossiana, Rome, Italy , November (1998) pp. 525-529.

